International Research Journal of Engineering and Technology (IRJET) e-ISSN: 2395-0056
Volume: 04 Issue: 07 | July -2017 www.irjet.net p-ISSN: 2395-0072

Synthesis, Spectroscopic (FT-IR, FT-Raman), first order hyperpolarizability and HOMO-LUMO analysis of (2E)-N-phenyl-3-(4H-pyran-4-yl) prop-2-enamide

S. Abbas Manthiri[1], R. Raj Muhamed[1*], V. Sathyanarayanamoorthi[2], R. Rajesh[3], M. Raja[1]

[1]Department of Physics, Jamal Mohamed College, Tiruchirappalli-620020, Tamil Nadu, India
[2]Post Graduate and Research Department of Physics, PSG College of Arts and Science, Coimbatore-641014, India
[3]Post Graduate and Research Department of Physics, Sri Vijay Vidyalaya College of Arts and Science for Woman, Dharmapuri-636807, India

---

Abstract - *In this work, the vibrational spectral analysis was carried out by using FT-Raman and FT-IR spectroscopy in the range 4000-100 cm-1 and 4000-400 cm-1 respectively, for (2E)-N-phenyl-3-(4H-pyran-4-yl)prop-2-enamid (P3P2E) molecule. Theoretical calculations were performed by density functional theory (DFT) method using 6-311++G(d,p) basis sets. The complete vibrational assignments of wavenumbers were made on the basis of potential energy distribution (PED). The results of the calculations were applied to simulated spectra of the title compound, which show excellent agreement with observed spectra. The frontier orbital energy gap and dipole moment illustrates the high reactivity of the title molecule. The first order hyperpolarizability (β0) and related properties (μ, α and Δα) of the molecule were also calculated. Molecular electrostatic potential (MEP) and HOMO-LUMO energy levels are also constructed. The thermodynamic properties of the title compound were calculated at different temperatures.*

Key Words: DFT, FT-IR, FT-Raman, NLO, MEP

1. INTRODUCTION

Enamides or enecarbamates are well-known versatile motifs in organic synthesis [1,2]. The π-donating ability of their nitrogen atom renders enamines more electron-rich [3] than simple enols or enol ethers, thereby predisposing them to electrophilic activation. However, enamines are highly sensitive toward hydrolysis, thereby creating serious difficulties in their experimental handling [4,5]. Consequently, the great potential of the chemistry of enamines has not been completely exploited. In this context, efforts have been directed towards the use of more stable enamines [6]. Enamides and enecarbamates that carry an electron-withdrawing group on the nitrogen were found to be ideal candidates. Indeed, enamides are commonly present in natural products and active drugs [7, 8] demonstrating their high stability.

The density functional theory (DFT) is a popular method for the calculation of molecular structures, vibrational frequencies and energies of molecules [6]. The density functional theory studies on the vibrational and electronic spectra of Enamides derivative (2E)-N-phenyl-3-(4H-pyran-4-yl)prop-2-enamid has not been carried out. Thus, in the present investigation, owing to the biological importance of substituted phenyl, an extensive experimental and theoretical studies of title compound has been undertaken by recording their FT-IR, FT-Raman spectra and subjecting them to potential energy distribution analysis for the proper assignment of the vibrational fundamentals. In addition, HOMO, LUMO analysis has been used to elucidate the information regarding charge transfer within the molecule.

2. METERIAL AND METHODS

2.1 Synthesis

A mixture of equimolar (0.01) concentration of finely powdered 1.35 g N-phenylacetamide and 1.10 g of 4H-pyran-4-carbaldehyde were dissolved in minimum amount of ethanol (30ml) taken in round bottom flask stir for 30 minutes. Sufficient 2N NaOH solution was added to the above solution and continuous stirring for 5 hrs in ice cold condition till yellow precipitate was formed. This was then neutralized with 2N HCl and dilutes with water and left overnight. The precipitate chalcones were filtered and washed with water and recrystallised from ethanol. The reaction scheme is given Fig 1

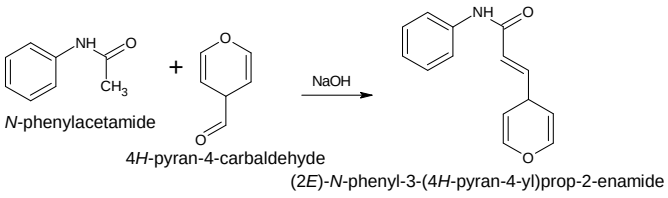

Fig -1: The scheme of the synthesis of P3P2E

2.2 Experimental details

The FT-IR spectrum of the synthesis compound (2E)-N-phenyl-3-(4H-pyran-4-yl)prop-2-enamid (P3P2E) was recorded in the region 4000-450 cm-1 in evacuation mode using a KBr pellet technique with 1.0 cm-1 resolution on a PERKIN ELMER FT-IR spectrophotometer. The FT-Raman

Table -2: Calculated vibrational frequencies (cm-1) assignments of P3P2E based on B3LYP/6-311++G(d,p)
aγ-stretching,γa-Symmetrical stretching,γas-asymmetrical stretching, β- bending , τ-torsion, vs-very strong, s- strong, m-

Mode no	Experimental wave number (cm-1)		Theoretical wave number(cm-1)		I_{IR} [c]	I_{RAMAN} [d]	Assignments (PED)[a,b]
	FTIR	FT-RAMAN	Unscaled	scaled			
84	-	-	3626	3485	4	26	γNH(100)
83	3127(s)	3128(s)	3245	3119	2	10	γCH (99)
82	-	3095(s)	3222	3096	1	52	γCH (92)
81	-	-	3219	3093	4	20	γCH (92)
80	3074(s)	-	3192	3067	4	61	γCH (99)
79	-	-	3184	3060	0	16	γCH (92)
78	-	-	3184	3059	1	12	γCH (92)
77	-	-	3177	3053	5	19	γCH (99)
76	-	3043(vw)	3168	3044	0	20	γCH (99)
75	-	-	3164	3040	2	18	γCH (99)
74	-	-	3148	3025	3	9	γCH (90)
73	2996(m)	2989(vw)	3112	2991	4	7	γCH (99)
72	2854(m)	2981(s)	2987	2871	5	21	γCH (100)
71	1666(vs)	1688(s)	1734	1666	56	100	γOC (46) + γCC (49)
70	-	1663(vs)	1729	1661	24	39	γOC (46) + γCC (40)
69	1608(vs)	1624(vw)	1680	1615	12	24	γOC (46) + γCC (58)
68	1594(vs)	-	1668	1603	10	1	γCC (40)
67		1592(vs)	1642	1578	11	64	γCC (32)
66	-	1546(s)	1634	1570	17	3	γCC (44) + βHNC(43)
65	1489(vs)	-	1562	1501	100	43	γNC (24) + βHNC(43)
64		1490(m)	1525	1466	19	11	βHCC(62)
63	1393(vs)	-	1468	1411	28	12	γCC (24) + βHCC(34)
62	1370(vs)	1372(vs)	1429	1373	0	1	βHCO(59)+ βHCC(47)
61	1314(vs)	1315(vs)	1375	1321	0	0	βHCO(59)
60	-	-	1357	1304	6	8	βHCC(86) + τHCCC(19)
59	-	-	1354	1301	11	12	βHCC(86) + τHCCC(19)
58	1291(vs)	1292(vs)	1340	1288	27	39	γCC (22) + βHCC(19)
57		1262(s)	1329	1277	1	1	βHCC(43) + τHCCC(19)
56	1259(vs)	-	1325	1273	0	7	γCC (58) + βHCC(73)
55	-	1236(s)	1281	1231	28	0	γOC (44) + βHCC(47)
54	-	-	1266	1217	4	6	γNC (19)+βHCC(30)+τHCCC(19)
53	-	-	1261	1212	24	63	γCC (14) + γNC (19) + βHNC(43)
52	-	1180(s)	1239	1191	3	10	βHCO(59)+ βHCC(47)
51	1169(s)	-	1226	1178	9	6	γNC (19) + γCC (19) + βHCC(30) + τHCCC(19)
50	-	-	1203	1156	2	8	βHCC(73)
49	1117(m)	1117(vs)	1183	1137	0	2	βHCC(64)
48	1089(vs)	1091(vs)	1112	1068	3	0	γCC (69) + βHCC(77)
47	-	-	1110	1067	16	0	γOC (21) +γCC (16) + βHCC(43)
46	1039(s)	-	1097	1054	8	0	γCC (62)
45	1008(vs)	1010(s)	1052	1011	1	4	γCC 45) + βHCC(11)
44	-		1026	986	2	2	βCCC(20)+ βCCO(31)
43	-		1013	974	0	13	βCCC(75)
42	967(s)	969(vs)	1006	967	1	0	τHCCN(32)+ τHCCC(41)
41	-		1003	964	0	0	τHCCC(94)+ τCCCC(11)
40	-		1000	961	10	0	γOC (23) + γCC (16) + τHCCN(32)
39	-		983	945	1	4	γNC (24) + γCC (19)
38	-		978	940	0	0	τHCCC(91)
37	-		960	922	0	0	τHCOC(62)+ τHCCO(62)
36	-		952	914	0	1	τHCOC(62)+ τHCCO(62)
35	-		930	894	21	1	γOC (44) + βCOC(23)
34	-		916	881	2	0	τHCCC(97)
33	-		897	862	4	3	γOC (44) + βOCC(41) + βCOC(23)
32	-	845(vs)	878	844	0	2	τHCCN(32)+ τHCCC(41)+Out ONCC(-20)
31	829(vs)		863	829	0	8	γCC (22) + γNC (19) +βCCC(26)+ βCCN(22)
30	-		841	808	0	0	τHCCC(99)
29	749(vs)		785	754	0	0	τHCOC(62)+ τHCCO(62)
28	-		772	741	21	0	τHCCO(62)
27	707(vs)		767	737	15	0	τHCCC(99)+ τCCCC(11)+Out NCCC(25)
26	-	709(vs)	707	680	1	1	βCCC(26)
25	-		707	680	1	0	τHCCN(32)+ τCCCC(31)+ Out ONCC(-20)
24	-		705	677	8	0	τHCCC(66)+ τCCCC(70)
23	-	632(vs)	650	624	2	3	τCCOC(19)+ τOCCC(-19)+ τCOCC(15)
22	-		648	623	0	1	βCCC(-13)+ βCCO(31)+ βOCC(41)
21	606(m)		632	607	0	1	βCCC(66)
20	535(w)		561	539	0	0	βCCC(39)+ βCOC(23)
19	-		540	519	2	1	βOCC(37)+ βCCC(17)+ βCOC(23)
18	506(s)		521	501	1	0	τHNCC(50)+Out NCCC(25)
17	-		515	495	12	0	τHNCC(50)+Out NCCC(25)
16	449(s)	451(m)	475	457	0	0	βCCC(14)+ τCCCC(43)+ τCCOC(19)+ τOCCC (-18)+ τCOCC(15)
15	-		453	435	7	1	βCCC(13)+ τCCOC(19)
14	-	381(s)	418	401	0	0	τHCCC(71)+ τCCCC(70)
13	-	355(s)	348	334	0	0	βCCC(17)+βCNC(26)+ βNCC(34)
12	-	301(s)	317	305	0	0	βCCC(14)+τOCCC(-18)+ τCCCC(31)
11	-		310	298	4	0	βOCC(37)+τCOCC(15)
10	-	271(vs)	253	243	0	0	τCCCC(70)+ τCCNC(15)
9	-		237	228	0	0	γCC (19) +βCCC(39)+ βCCN(22)
8	-	169(s)	182	175	1	0	βCCC(13)+βCNC(26)+ βNCC (34)
7	-	150(vs)	142	137	1	0	τCCCC(68)
6	-		89	85	0	0	βCCC(13)+βCNC(26)+ βCCN (22) +τCCCC(43)+ τCOCC(15)
5	-		56	54	1	0	τCNCC(45)+ τCCCC(68)
4	-		50	48	0	0	τCCCN(-17)+ τCNCC(45)+τCCCC(37)
3	-		37	36	0	1	τCCNC(51)+τCCCC(31)+OutNCCC(25)
2	-		37	36	0	1	βCCC(52)+τCCCC(43)
1	-		16	15	1	0	τCCCN(-17)+τCCOC(37)

3.4 Frontier molecular orbitals (FMOs)

The highest occupied molecular orbitals (HOMOs) and the lowest-lying unoccupied molecular orbitals (LUMOs) are named as frontier molecular orbitals (FMOs). The FMOs play an important role in the optical and electric properties, as well as in quantum chemistry and UV–vis. spectra [25]. HOMO-LUMO orbitals are also called frontier orbitals as they lie at the outermost boundaries of the electrons of the molecules. The frontier orbital gap helps characterize the chemical reactivity and the kinetic stability of the molecule. A molecule with a small frontier orbital gap is generally associated with a high chemical reactivity, low kinetic stability and is also termed as soft molecule [25]. The 3D plots of the frontier orbitals HOMO and LUMO figures for the P3P2E are shown in Fig. 5. The lowest unoccupied molecular orbital (LUMO) energy is -1.8389 eV and the highest occupied molecular orbital (HOMO) energy is -6.2790 eV. Lower value in the HOMO and LUMO energy gap explains the eventual charge transfer interactions taking place within the molecule, which influences the biological activity of the molecule. The narrow energy gap between HOMO and LUMO facilitates intra molecular charge transfer which makes the material to be NLO active [50]. Analysis of the wavefunction indicates that the electron absorption corresponds to the transition from the ground to the first excited state and is mainly described by one-electron excitation from the HOMO to the LUMO. All the HOMO and LUMO have nodes. The positive phase is red and the negative one is green. By using HOMO and LUMO energy values for a molecule, the chemical hardness, electronegativity, chemical potential and electrophilicity index of the molecule were calculated. The calculated results are presented in Table 4. Considering the chemical hardness, if a molecule has large HOMO–LUMO gap, it is a hard molecule or small HOMO–LUMO gap it is a soft molecule. One can also relate the stability of molecule to hardness, which means that the molecule with least HOMO–LUMO gap means it is more reactive.

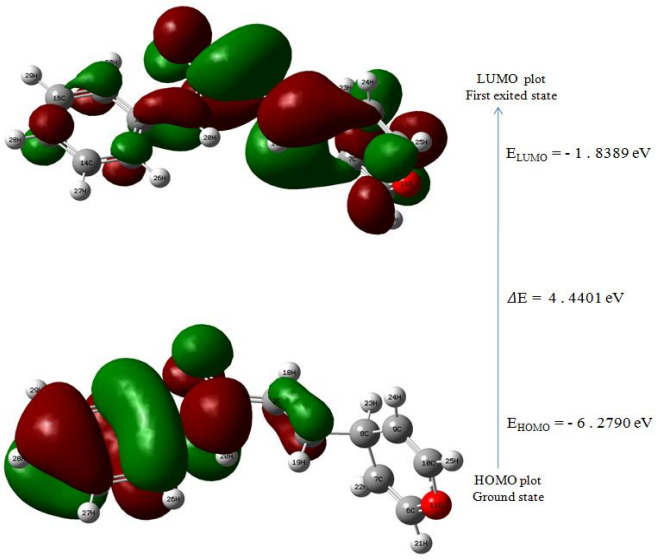

Fig -5: Highest occupied and lowest unoccupied molecular orbital of P3P2E obtain with B3LYP/6-311++G(d,p) method

3.5 Molecular electrostatic potential (MEP)

MEP and electrostatic potential are useful quantities to illustrate the charge distributions of molecules and used to visualize variably charged regions of a molecule. Therefore, the charge distributions can give information about how the molecules interact with another molecule. MEP is widely used as a reactivity map displaying most probable regions for the electrophilic attack of charged point-like reagents on organic molecules [26]. The molecular electrostatic potential V(r) that is created in the space around a molecule by its nuclei and electrons is well established as a guide to molecular reactive behavior. It is defined by:

$$V(r) = \sum Z_A \ / (R_A - r) \ - \int \rho(r')/(r'-r)dr'$$

Where the summation runs over all the nuclei A in the molecule and polarization and reorganization effects are neglected. ZA is the charge of the nucleus A, located at RA and ρ(r') is the electron density function of the molecule.

At any given point r(x, y, z) in the vicinity of a molecule, the MEP, V(r) is defined in terms of the interaction energy between the electrical charge generated from the molecule electrons and nuclei and a positive test charge (a proton) located at r [27]. The MEP is related to electron density and a very useful descriptor for determining sites for electrophilic attack and nucleophilic reactions as well as hydrogen-bonding interactions [28, 29]. To predict reactive sites for electrophilic and nucleophilic attack for the investigated molecule, the 3D Molecular electrostatic potential surface (MEPs) for the title molecule are shown in Figs. 6. The different values of the electrostatic potential at the surface are represented by different colors. Potential increases in the order red < orange < yellow < green < blue. The negative (red, orange and yellow) regions of the MEP are related to electrophilic reactivity. The MEP map shows that the negative potential sites are on electronegative oxygen atoms (O4 and O11) and the positive potential sites are around the hydrogen atoms. These sites give information about the region from where the compound can have intermolecular interactions. This predicted the most reactive site for both electrophilic and nucleophilic attack.

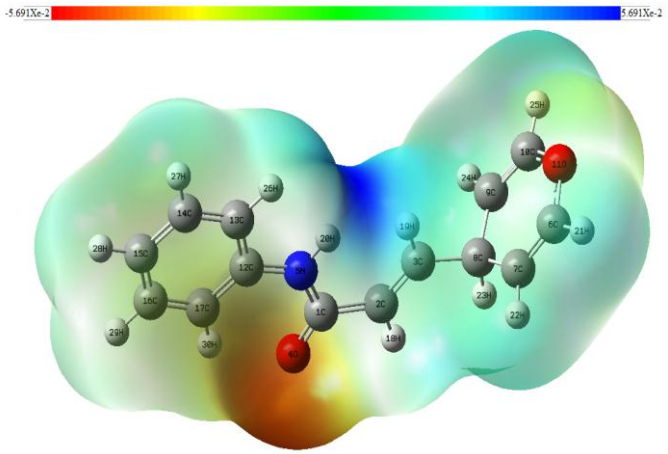

Fig -6: Molecular electrostatic potential of P3P2E calculated at B3LYP/6-311++G(d,p) basis set

3.6 Thermodynamic properties

On the basis of vibrational analysis at B3LYP/6-311++G(d,p) level, the standard statistical thermodynamic functions: heat capacity (C), entropy (S) and enthalpy (H) for the title compound were obtained from the theoretical harmonic frequencies and listed in Table 5. From Table 5, it can be observed that these thermodynamic functions are increasing with temperature ranging from 100 K to 700 K due to the fact that the molecular vibrational intensities increase with temperature [30]. The correlation equations between heat capacity, entropy, enthalpy and temperatures were fitted by quadratic formulas, and the corresponding fitting factors (R2) for these thermodynamic properties are 0.9997, 0.9999 and 0.9997, respectively. The corresponding fitting equations are as follows and the correlation graphics of those are shown in Fig. 7.

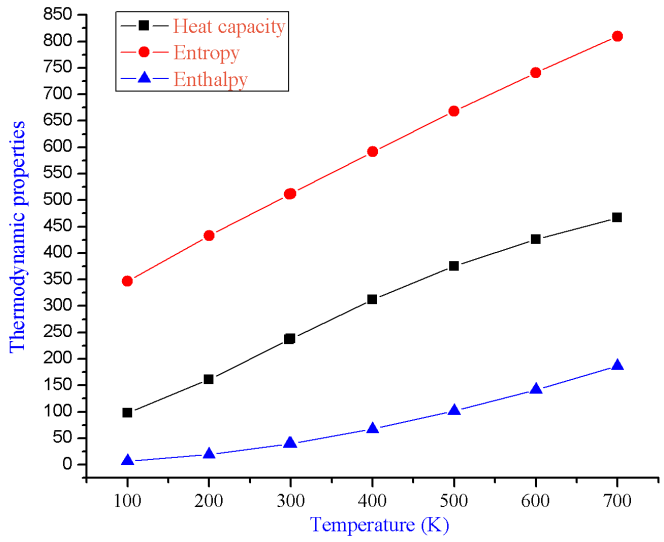

Fig -7: Correlation graphic of heat capacity, entropy, enthalpy and temperature for P3P2E

Table -4: Calculated energy values of title compound by B3LYP/6-311++G(d,p) method.

Basis set	B3LYP/6-311++G(d,p)
E_{Homo}(eV)	-6.279
E_{Lumo}(eV)	-1.8389
Ionization potential	6.279
Electron affinity	1.8389
Energy gap(eV)	4.4401
Electronegativity	4.05895
Chemical potential	-4.05895
Chemical hardness	2.22005
Chemical softness	0.22522
Electrophilicity index	3.710519

$\left(C^{0}_{p,m}\right)$ = 6.1678 + 0.8755T – 3.0162 x $10^{-4}T^2$ (R^2 = 0.9997)

$\left(S^{0}_{m}\right)$ = 259.6499 + 0.8890T –1.4608 x $10^{-4}T^2$(R^2 = 0.9999)

$\left(H^{0}_{m}\right)$ = - 0.9842 + 0.0387T – 3.2910 x $10^{-4}T^2$ (R^2 = 0.9997)

All the thermodynamic data supply helpful information for the further study on the P3P2E. They can be used to compute the other thermodynamic energies according to relationships of thermodynamic functions and estimate directions of chemical reactions according to the second law of thermodynamics in thermo chemical field [30]. It must be noticed that all thermodynamic calculations were done in gas phase and they could not be used in solution.

Table -5: Temperature dependence of thermodynamic properties of P3P2E at B3LYP /6-311++G(d,P)

T(K)	$C^{0}_{p,m}$ (J/ mol K)	S^{0}_{m} (J/ mol K)	H^{0}_{m} (kJ/ mol)
100	98.04	346.73	6.86
200	161.09	432.97	19.66
298.15	236.39	511.13	39.12
300	237.83	512.59	39.56
400	312.25	591.42	67.14
500	375.11	668.09	101.61
600	425.75	741.13	141.75
700	466.47	809.92	186.43

4. CONCLUSIONS

FT-IR, FT-Raman and DFT quantum chemical calculations studies were performed on P3P2E, in order to identify its structural and spectroscopic features. Several properties were carried out using experimental techniques and tools derived from DFT. On the basis of experimental results and PED calculations, assignments of all the fundamental vibrational frequencies were done. A good correlation between the observed and scaled wavenumbers was obtained for the title compound. Scaled results seemed to be in good agreement with experimental ones. HUMO and LUMO orbitals have been visualize. It has been conclude that the lowest singlet excited state of the title molecule is mainly derived from the HOMO-LUMO electron transition. The electric dipole moment, polarizability, mean polarizability and the first order hyperpolarizability of the title compound were calculated. The correlations of the statistical thermodynamics according to temperature were also presented. We hope our results will be of assistance in the quest of the experimental and theoretical evidence for the title molecule in reaction intermediates, nonlinear optical and photoelectric materials and will also be helpful for the design and synthesis of new materials.

REFERENCES

[1] R. Matsubara, S. Kobayashi, “Enamides and Enecarbamates as Nucleophiles in Stereoselective C–C and C–N Bond-Forming Reactions”, Acc. Chem. Res, 41 (2008) 292-301.

[2] D.R. Carbery, "Enamides: valuable organic substrates", Org. Biomol. Chem. 6 (2008) 3455-3460.

[3] H. Mayr, "Structure–Nucleophilicity Relationships for Enamines", Chem. Eur. J. 2003, 9, 2003, 2209-2218.

[4] O. Èervinka, In The Chemistry of Enamines, Part 1; Rappoport, Z., Ed.; John Wiley & Sons: New York, 1994, Chap. 9, 467.

[5] G. Bélanger, M. Doré, F. Ménard, V.J. Darsigny, "Reactions of Aldehydes and Ketones and their Derivatives", Org. Chem, 71, 2006, 7481.

[6] S. Mukherjee, J.W. Yang, S. Hoffmann, "Asymmetric enamine catalysis", B List. Chem. Rev. 2007, 107, 5471-5569.

[7] T. Kuranaga, Y. Sesoko, M. Inoue, "Cu-mediated enamide formation in the total synthesis of complex peptide natural products", Nat. Prod. Rep, 31, 2014, 514-532.

[8] K. Okamoto, M. Sakagami, F. Feng, H. Togame, H. Takemoto, S. Ichikawa, A. Matsuda, "Total synthesis of pacidamycin D by Cu (I)-catalyzed oxy enamide formation", A. Org. Lett, 13, 2011, 5240-5243.

[9] K. Golcuk, A. Altun, M. Kumru, "Thermal studies and vibrational analyses of m-methylaniline complexes of Zn (II), Cd (II) and Hg (II) bromides", Spectrochim. Acta 59A (2003) 1841–1847.

[10] M. J. Frisch, G. W. Trucks, H. B. Schlegel, Gaussian 09, Revision **E.01,** Gaussian, Inc., Wallingford CT, 2009.

[11] N. Sundaraganesan, S. Illakiamani, H. Saleem, P.M. Wojciechowski, D. Michaliska, "FT-Raman and FT-IR spectra, vibrational assignments and density functional studies of 5-bromo-2-nitropyridine", Spectrochim. Acta A 61 (2005) 2995-3001.

[12] M.H. Jamroz, "Vibrational energy distribution analysis (VEDA): scopes and limitations", Spectrochim. Acta A 114 (2004) 220-230.

[13] A.M. Asiri, M. Akkurt, S. A. Khan, I. Ullah Khan and M.N. Arshad, "(E)-2-Cyano-3-[4-(dimethylamino)phenyl]- N -phenylprop-2-enamide", Acta Cryst. (2009). E65, o1303.

[14] N. Swarnalatha, S.Gunasekaran, S. Muthu, M. Nagarajan, "Molecular structure analysis and spectroscopic characterization of 9-methoxy-2H-furo[3,2-g]chromen-2-one with experimental (FT-IR and FT-Raman) techniques and quantum chemical calculations", spectrochim. Acta part A 137 (2015) 721-729.

[15] L.G. Wade (Ed), Advanced Organic Chemistry, 4th ed., Wiley, New York,1992. p.723.

[16] N. Sundaraganesan, S.Illakiamani, C. Meganathan, B.D. Joshua, "Vibrational spectroscopy investigation using ab initio and density functional theory analysis on the structure of 3-aminobenzotrifluoride", Spectrochim. Acta A 67 (2007) 214-224.

[17] Silverstein, G.C. Basseler, C. Morill, Spectrometric Identification of Organic Compounds, Wiley, New York, 1981.

[18] T. Gnanasambandan, S. Gunasekaran, and S. Seshadri, "Vibrational spectroscopic investigation on propylthiouracil, International Journal of Recent Scientific Research", 3 (2012) 590 – 597

[19] G. Varsanyi, Vibrational Spectra of Benzene Derivatives, Academic Press, NewYork, 1969.

[20] M. Raja, R. Raj Muhamed, S. Muthu, M. Suresh, "Synthesis, spectroscopic (FT-IR, FT-Raman, NMR, UV-Visible), NLO, NBO, HOMO-LUMO, Fukui function and molecular docking study of (E)-1-(5-bromo-2-hydroxybenzylidene)semicarbazide", Journal of Molecular Structure, 1141 (2017) 284–298.

[21] M. Szafran, A. komasa, E.B. Adamska, "Crystal and molecular structure of 4-carboxypiperidinium chloride (4-piperidinecarboxylic acid hydrochloride)", J Mol. Struct. THEOCHEM 827 (2007) 101-107.

[22] K.S. Thanthiri Watte, K. M. Nalin de silva, "Non-linear optical properties of novel fluorenyl derivatives-ab initio quantum chemical calculations", J. Mol. Struct. Theochem. 617 (2002) 169-175.

[23] S.G. Sagdinc, A. Esme, Spectrochim. "Theoretical and vibrational studies of 4, 5-diphenyl-2-2 oxazole propionic acid (oxaprozin)", Acta Part A 75 (2010) 1370-1380.

[24] S. Muthu, G. Ramachandran, "Spectroscopic studies (FTIR, FT-Raman and UV–Visible), normal coordinate analysis, NBO analysis", first order hyper polarizability, HOMO and LUMO analysis of (1R)-N-(Prop-2-yn-1-yl)-2,3-dihydro-1H-inden-1-amine molecule by ab initio HF and density functional methods Spectrochim. Acta part A 121, 2014, 394-403.

[25] I. Fleming, Frontier Orbitals and Organic Chemical Reactions, John Wiley & Sons, New York, 1976.

[26] P. Politzer, D.G. Truhlar (Eds.), Chemical Application of Atomic and Molecular Electrostatic Potentials, Plenum, New York, 1981.

[27] P. Politzer, J.S. Murray, "The fundamental nature and role of the electrostatic potential in atoms and molecules", Theor. Chem. Acc. 108, 2002, 134–142.

[28] F.J. Luque, J.M. Lopez, M. Orozco, "Perspective on Electrostatic interactions of a solute with a continuum. A direct utilization of ab initio molecular potentials for the prevision of solvent effects" Theor. Chem. Acc. 103, 2000, 343–345.

[29] N. Okulik, A.H. Jubert, "Theoretical analysis of the reactive sites of non-steroidal anti-inflammatory drugs", Internet Electron. J. Mol. Des. 4, 2005, 17–30.

[30] B. Otto, J. Boerio-Goates, Chemical Thermodynamics: Advanced Applications, Calculations from Statistical Thermodynamics, Academic Press, 2000.